J|A|C|S
ARTICLES
Published on Web 09/26/2006

Amorphous Linear Aliphatic Polyesters for the Facile Preparation of Tunable Rapidly Degrading Elastomeric Devices and Delivery Vectors

David A. Olson, Stephanie E. A. Gratton, Joseph M. DeSimone, and Valerie V. Sheares*

Contribution from the Department of Chemistry, University of North Carolina at Chapel Hill, Venable Hall CB 3290, Chapel Hill, North Carolina 27599-3290

Received May 3, 2006; E-mail: ashby@email.unc.edu

Abstract: A versatile method for preparing amorphous degradable elastomers with tunable properties that can be easily fabricated into a wide variety of shape-specific devices was investigated. Completely amorphous, liquid poly(ester ether) prepolymers with number-average molecular weights between 4 and 6×10^3 g/mol were prepared via condensation polymerization. These liquid prepolymers were then thermally cross-linked to form degradable elastomeric structures. The ability to vary the composition of these liquid prepolymers allows for easy control of the mechanical and degradation properties of the resulting elastomeric structures. Materials can be designed to completely degrade in vitro over a range of 30 days to 6 months, while the Young's modulus can be varied over 3 orders of magnitude ($G = 0.02-20$ MPa). Also, the liquid nature of these prepolymers makes them amenable to a wide variety of fabrication techniques. Using traditional and modified imprint lithography techniques, we have fabricated devices that demonstrate a wide variety of biologically applicable topologies, which could easily be extended to fabricate devices with more complex geometries. Until now, no method has combined this ease and speed of fabrication with the ability to control the mechanical and degradation properties of the resulting elastomers over such a broad range.

Introduction

Poly(L-lactic acid), poly(glycolic acid), and poly(ϵ-caprolactone) are the most commonly used degradable polyester materials for today's biomedical applications.[1,2] While numerous elegant examples of their preparation exist, these materials suffer from the inherent drawback that they are crystalline, hydrophobic, and possess a very small window within which their mechanical properties can be varied. Crystalline materials generally swell and deform significantly upon degradation. Moreover, crystallinity results in lower diffusion coefficients of solvents through the material, which hinders the ability of water molecules to diffuse into the material and attack the hydrolytically labile ester bonds.[3−6] As a result, degradation rates are on the order of 6 months to several years.

Besides reducing degradation rates, crystallinity also produces a hard material with low resilience. Many biomedical applications, such as soft tissue regeneration or engineering scaffolds[7−12] and drug delivery systems,[13−16] require soft materials capable of withstanding dynamic environments. Polyester-based cross-linked elastomeric materials offer an improved option for these applications. If properly designed, the elastomeric network can provide a soft, mechanically stable structure in dynamic environments, while still possessing the ability to degrade. It is especially advantageous that these elastomeric networks be completely amorphous. Completely amorphous, low T_g materials will have much higher diffusion coefficients for solutes dispersed or dissolved in them as compared to crystalline materials, which will give rise to different release profiles. In addition, the permeability of biological fluids in such materials should also allow them to degrade more rapidly.

An ideal bioelastomer should be prepared using a synthetic methodology that allows for the: (1) preparation of a completely amorphous elastomer, (2) ability to easily design a wide variety

(1) Uhrich, K. E.; Cannizzaro, S. M.; Langer, R. S.; Shakesheff, K. M. *Chem. Rev.* **1999**, *99*, 3181−3198.
(2) Wang, Y.; Ameer, G.; Sheppard, B.; Langer, R. S. *Nat. Biotechnol.* **2002**, *20*, 602−606.
(3) Vert, M.; Mauduit, J.; Li, S. *Biomaterials* **1994**, *15*, 1209−1213.
(4) Slager, J.; Domb, A. J. *Adv. Drug Delivery Rev.* **2003**, *55*, 549−583.
(5) Alexis, F. *Polym. Int.* **2005**, *54*, 36−46.
(6) Bigg, D. M. *Adv. Polym. Technol.* **2005**, *24*, 69−82.
(7) Amsden, B. G.; Misra, G.; Gu, F.; Younes, H. M. *Biomacromolecules* **2004**, *5*, 2479−2486.
(8) Holland, T. A.; Tabata, Y.; Mikos, A. G. *J. Controlled Release* **2005**, *101*, 111−125.
(9) Pego, A. P.; Poot, A. A.; Grijpma, D. W.; Feijen, J. *J. Controlled Release* **2003**, *87*, 69−79.
(10) Helen, H. L.; Saadiq, F. E.; Kimberli, D. S.; Cato, T. L. *J. Biomed. Mater. Res. A* **2003**, *64*, 465−474.
(11) Sodian, R.; Sperling, J. S.; Martin, S. P.; Egozy, A.; Stock, U.; E., M. J. *Tissue Eng.* **2000**, *6*, 183−188.
(12) Hinrichs, W. L.; Kuit, J.; Feil, H.; Wildevuur, C. R.; Feijen, J. *Biomaterials* **1992**, *13*, 585−593.
(13) Albertsson, A.-C.; Edlund, U.; Stridsberg, K. *Macromol. Symp.* **2000**, *157*, 39−46.
(14) Peppas, N. A.; Langer, R. *Science* **1994**, *263*, 1715−1720.
(15) Pitt, C. G.; Hendren, R. W.; Schindler, A.; Woodward, S. C. *J. Controlled Release* **1984**, *1*, 3−14.
(16) Pitt, C. G.; Gu, Z. W.; Ingram, P.; Hendren, R. W. *J. Polym. Sci., Part A: Polym. Chem.* **1987**, *25*, 955−966.

of simply processable materials from readily available starting materials, (3) precise control of the degradation rates of the materials over a wide range, (4) precise control of the mechanical properties of the materials over a wide range, (5) preparation of a material that is biocompatible, and (6) easy fabrication of the prepolymer into a wide range of device structures, including complex geometries. To date, there is no synthetic methodology that can simultaneously satisfy all six of these requirements.

Two classes of synthetic bioelastomer exist: thermoplastic[17−23] and thermoset.[2,7,12,24−33] While thermoplastic elastomer materials offer synthetic control and ease of processing, the majority of these materials contain crystalline domains. This not only reduces the degradation rates, it also leads to a material that degrades heterogeneously. Thermoset elastomer materials that are currently described in the literature offer the advantage of either being completely amorphous, or semicrystalline, with melting transitions below physiological temperatures. Optimal elastic mechanical and degradation properties for semicrystalline elastomers are achieved when the material is above its T_m and as such above its T_g. However, they suffer from a lack of ability to vary properties by controlling the cross-linking chemistry, which also limits the ability to process the materials into complex geometric shapes.[2,12,24−27,34] In addition, some of these multifunctional monomers are synthetically challenging to prepare and require extended curing times (as long as 6 days), which is a drawback from a commercialization standpoint.[2,25,27−30,34] Some examples of controlled network formation do exist, but they employ postpolymerization functionalization reactions that are tedious and can potentially degrade the materials.[7,31,33] Furthermore, many of these examples employ the use of complex polymeric structures, such as star or branched polymers, which are synthetically challenging to control. While hydrogels, a class of thermoset materials, offer several advantages, most suffer from limited mechanical properties and require hydration.[35,36] Regardless of the techniques used to form the network, the processing options for all of these thermoset materials are severely limited due to the fundamental nature of their preparation.

Here, we report a hybrid class of completely amorphous degradable elastomeric thermoset materials that combine the advantages of amorphous thermoset materials with the synthetic and processing advantages of thermoplastic elastomer materials. The essential feature that allows for this combination of advantages is the use of a completely amorphous linear prepolymer that has a low glass transition temperature and is liquid at room temperature. These prepolymers contain cross-linkable groups, incorporated during polymerization, which can be subsequently used to form elastomeric networks that can be subsequently degradable. The prepolymers are completely amorphous, and therefore the resulting elastomeric networks are necessarily amorphous. This leads to elastomeric materials that degrade extremely rapidly, due to the increased coefficient of diffusion, with materials degrading completely in as little as 30 days. Furthermore, these amorphous prepolymers are prepared from facile polycondensation polymerization techniques. This offers the ability to precisely control the composition of the resulting prepolymers and hence the network structure of the resulting elastomers. As a result, the degradation rates and mechanical properties of the resulting cross-linked networks can be precisely controlled over a wide range. Even more advantageous from a processing standpoint, the liquid prepolymers can be easily fabricated or molded into a wide array of devices and shapes.

Results and Discussion

An amorphous linear prepolymer with a glass transition temperature well below room temperature that is a liquid at room temperature is essential for the type of hybrid approach previously described. Previous investigations in our laboratory discovered a class of amorphous poly(ester ether) materials prepared from the condensation polymerization of HMA and diethylene glycol.[37] The amorphous nature, low glass transition temperature, and ability to cross-link these materials make them good candidates for preparing elastomeric materials. Furthermore, because these elastomeric materials contain hydrolytically unstable ester bonds, they are degradable. The desire for elastomers with precisely tailorable mechanical and degradation properties has led us to prepare a series of poly(ester ether) homopolymer materials from the condensation polymerization of HMA and ethylene glycol dimers (2EG), trimers (3EG), and tetramers (4EG). Homopolymers with number-average molecular weights near 5.0×10^3 g/mol were prepared, with molecular weights slightly increasing as the length of the EG oligomer increased (Scheme 1, Table 1). Novozyme-435, consisting of lipase B from *Candida antarctica* immobilized on a Lewatit macroporous resin, and $Sn(Oct)_2$ were both investigated as catalysts. Both catalysts produced polymers with similar number average molecular weights and thermal properties, with the Novozyme-435 offering a completely metal-free synthetic option. Glass transition temperatures were all below −30 °C with the EG oligomer length not having a significant effect.

Polycondensation techniques also allow for the facile preparation of random copolymer materials (Scheme 2). Diethylene glycol was used as the diol for all of these investigations. Materials with number-average molecular weights near 4.0 ×

(17) Cohn, D.; Hotovely Salomon, A. *Biomaterials* **2005**, *26*, 2297−2305.
(18) Loefgren, A.; Renstad, R.; Albertsson, A. C. *J. App. Polym. Sci.* **1995**, *55*, 1589−1600.
(19) Cohn, D.; Younes, H. M. *Biomaterials* **1989**, *10*, 466−477.
(20) Cohn, D.; Stern, T.; Gonzalez, M. F.; Epstein, J. *J. Biomed. Mater. Res.* **2002**, *59*, 273−281.
(21) Loefgren, A.; Albertsson, A. C.; Dubois, P.; Jerome, R.; Teyssie, P. *Macromolecules* **1994**, *27*, 5556−5562.
(22) Wada, R.; Hyon, S.; Nakamura, T.; Ikada, Y. *Pharm. Res.* **1991**, *8*, 1292−1296.
(23) Pitt, C. G.; Jeffcoat, A. R.; Zweidinger, R. A.; Schindler, A. *J. Biomed. Mater. Res.* **1979**, *13*, 497−507.
(24) Wang, Y.; Kim, Y. M.; Langer, R. *J. Biomed. Mater. Res.* **2003**, *66A*, 192−197.
(25) Yang, J.; Webb, A.; Ameer, G. *Adv. Mater.* **2004**, *16*, 511−516.
(26) Liu, Q.; Tian, M.; Ding, T.; Shi, R.; Zhang, L. *J. Appl. Polym. Sci.* **2005**, *98*, 2033−2041.
(27) Ding, T.; Liu, Q.; Shi, R.; Tian, M.; Yang, J.; Zhang, L. *Polym. Degrad. Stab.* **2006**, *91*, 733−739.
(28) Amsden, B. G.; Wang, S.; Wyss, U. *Biomacromolecules* **2004**, *5*, 1399−1404.
(29) Palmgren, R.; Karlsson, S.; Albertsson, A.-C. *J. Polym. Sci., Part A: Polym. Chem.* **1997**, *35*, 1635−1649.
(30) Younes, H. M.; Bravo-Grimaldo, E.; Amsden, B. G. *Biomaterials* **2004**, *25*, 5261−5269.
(31) Amsden, B. G.; Tse, M. Y.; Turner, N. D.; Knight, D. K.; Pang, S. C. *Biomacromolecules* **2006**, *7*, 365−372.
(32) Nagata, M.; Sato, Y. *Polymer* **2003**, *45*, 87−93.
(33) Turunen, M. P.; Korhonen, H.; Touminen, J.; Seppala, J. *Polym. Int.* **2001**, *51*, 92−100.
(34) Bettinger, C. J.; Orrick, B.; Misra, A.; Langer, R.; Borenstein, J. T. *Biomaterials* **2006**, *27*, 2558−2565.
(35) Temenoff, J. S.; Athanasiou, K. A.; LeBaron, R. G.; Mikos, A. G. *Biomed. Mater. Res.* **2002**, *59*, 429−437.
(36) Lee, K. Y.; Rowley, J. A.; Eiselt, P.; Moy, E. M.; Bouhadir, K. H.; Mooney, D. J. *Macromolecules* **2000**, *33*, 4291−4294.
(37) Olson, D. A.; Sheares, V. V. *Macromolecules* **2006**, *39*, 2808−2814.

Scheme 1. Synthesis of Unsaturated Poly(ester ether) Prepolymers

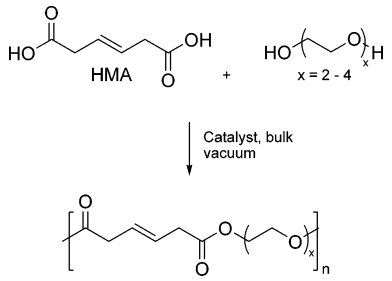

Table 1. Characterization of Poly(ester ether) Prepolymers

prepolymer	EG diol	$\langle M_n \rangle \times 10^{-3}$ (g/mol)[a]	PDI[a]	T_g (°C)[b]	weight loss (°C)[c] 5%	10%
1	2[d]	4.9	1.7	−33	302	326
2	3[d]	4.9	1.9	−33	274	316
3	4[d]	5.6	1.8	−36	301	319
4	2[e]	6.4	1.2	−32	298	319

[a] Determined by GPC. [b] Determined by DSC, second heat, 10 °C/min. [c] Determined by TGA in N_2, 10 °C/min. [d] 1.0 mol % $Sn(Oct)_2$ catalyst, 24 h. [e] 10.0 wt % Novozyme-435 catalyst, 48 h.

Scheme 2. Synthesis of Unsaturated Poly(ester ether) Copolymers

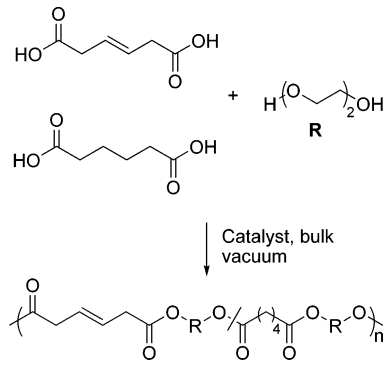

10^3 g/mol were prepared (Table 2). Observed monomer incorporation was identical to the ratio of monomers in the polymerization feed. Copolymers demonstrated a window of glass transition temperatures ranging from −45 to −30 °C. Yields were above 96% for all materials. By diluting out the amount of HMA in the material with AA, the amount of cross-linkable groups in the material was subsequently reduced. This allowed for control over the cross-linking densities of the subsequent cross-linked elastomer materials. There are very few examples of materials in the literature that afford this combination of synthetic ease and control for the preparation of a prepolymer material.[7,31,32]

Clearly, the manner of the distribution of the two diacid monomers (random or segmented) will have an effect on the network structure and hence the mechanical properties of the elastomer materials. As a result, the distribution of these two monomers was investigated. This was investigated by monitoring a copolymerization reaction where the molar ratio of the two diacid monomers was equal (0.5:0.5:1). The incorporation of the two monomers was monitored via ^{1}H NMR during polymerization (Figure 1). Subsequently, the relative ratios of the respective polymer to monomer peak integrals were plotted versus time (Figure 2). This plot shows that HMA ($k = 0.78 \pm 0.09$) and adipic acid ($k = 0.62 \pm 0.08$) are being incorporated into the copolymer at similar rates.

The thermal properties of prepolymers **5**−**10** were also used to investigate the nature of the incorporation of HMA and AA. First, all of the copolymers prepared display a single, clear glass transition temperature (Table 2). Second, a derivative of the Fox equation for random copolymers can be applied to this series of copolymers, where w_1 and w_2 are the respective fractions of the two monomers, and T_{g1} and T_{g2} are the glass transition temperatures of the homopolymers prepared from the respective monomers:

$$T_g = w_1 T_{g1} + w_2 T_{g2}$$

The plot of the transition temperatures predicted by the Fox equation is in very close agreement with the transition temperature measured experimentally (Figure 3), further supporting that the copolymers prepared are random in nature.

Once the liquid amorphous linear prepolymer materials were prepared, cross-linking of these materials was explored. Initially, benzoyl peroxide (BPO) was used as the free radical initiator. Initiator concentration, curing time, and curing temperature were all varied to investigate the effect that each had on the sol fraction (Q_s) of the resulting material (Figure 4). All of these studies were performed on prepolymer **1**. Soluble fractions decreased as the initiator concentration increased from 0.5 to 10.0 wt % at a curing temperature of 115 °C (Figure 4A). Similarly, they decreased as the curing time increased from 6 to 24 h, again at a curing temperature of 115 °C. At 24 h of curing, materials demonstrate similar soluble fractions regardless of initiator concentration. Finally, the curing temperature was varied from 115 to 160 °C using 5.0 wt % BPO and a curing time of 24 h in all cases (Figure 4B). Soluble fractions again noticeably decreased as the curing temperature increased; however, curing temperatures above 130 °C yielded films that were significantly yellowed.

Based on the above results, curing conditions of 5.0 wt % BPO, 130 °C for 24 h were subsequently investigated. The thermal and mechanical properties of elastomers prepared from HMA:*n*EG prepolymers, including materials prepared via enzyme catalysis, using these curing conditions were characterized. Cross-linking raised the glass transition temperatures of the materials to between −10 and −20 °C, with materials prepared from 4EG demonstrating the lowest transition temperature (Table 3, elastomer 5). Cross-linking densities steadily decreased as the EG length increased, resulting from a lower concentration of double bonds in the backbone of the material (Table 3). The soluble fractions follow a similar trend. Correspondingly, the Young's modulus (G) and ultimate stress (ϵ) of the materials decreased slightly as the EG length increased, while the ultimate extension (σ) increased. While changing the EG length did offer a limited ability to modify the mechanical properties of the elastomeric materials, the ability to prepare materials with a wider range of mechanical properties was of interest.

As previously discussed, the ideal degradable bioelastomer should be prepared using a synthetic methodology that allows for the precise control of mechanical properties over a broad range. Three approaches to demonstrate the ability of our methodology to do so were undertaken. First, the copolymeric prepolymers prepared above were cross-linked. Second, the use

Table 2. Characterization of HMA:AA Copolymers

prepolymer	HMA:AA:DEG ratio targeted	HMA:AA:DEG ratio observed[a]	$\langle M_n \rangle \times 10^{-3}$ (g/mol)[b]	PDI[b]	T_g (°C)[c]	weight loss (°C)[d] 5%	weight loss (°C)[d] 10%
5	0:50:50	0:50:50	3.3	1.9	−46	268	290
6	10:40:50	10:40:50	4.3	1.7	−44	322	340
7	20:30:50	20:30:50	3.9	1.7	−40	314	337
8	30:20:50	30:20:50	4.1	1.7	−37	298	326
9	40:10:50	40:10:50	4.0	1.7	−33	300	318
10	50:0:50	50:0:50	4.9	1.7	−31	302	326

[a] Determined by ^{1}H NMR. [b] Determined by GPC. [c] Determined by DSC, second heat, 10 °C/min. [d] Determined by TGA in N_2, 10 °C/min.

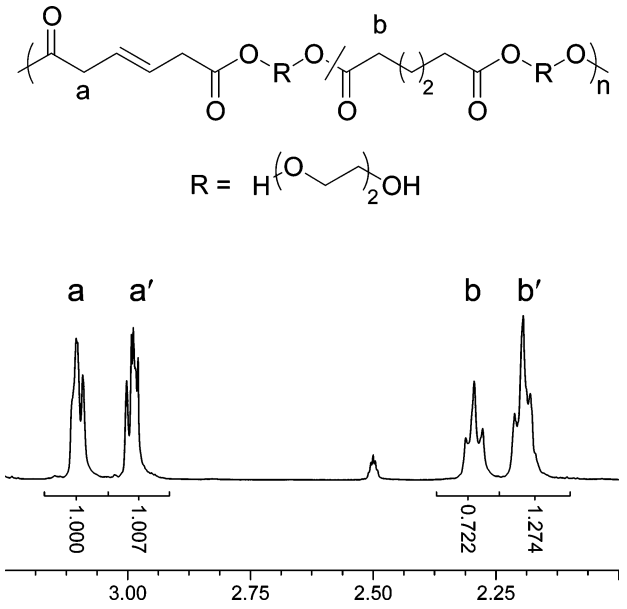

Figure 1. ^{1}H NMR peaks of HMA:AA copolymer used to determine monomer incorporation, after 1 h of reaction time (prime (′) sign denotes monomer proton).

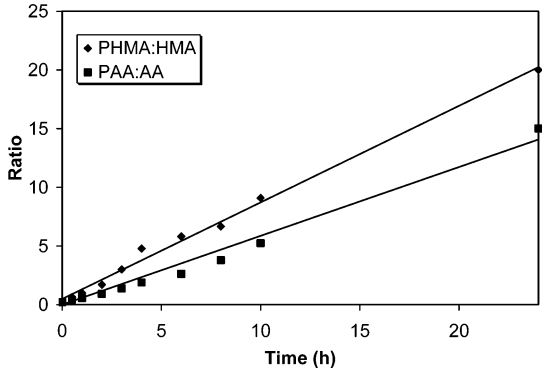

Figure 2. Characterization of monomer incorporation into HMA:AA copolymers as determined by ^{1}H NMR (where PHMA and PAA are the amounts of the respective monomers that have been incorporated into the copolymer).

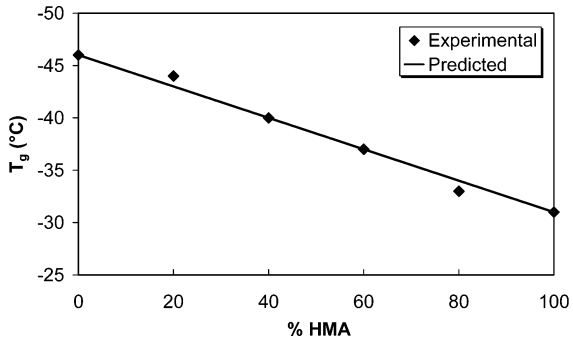

Figure 3. Glass transition temperature of HMA:AA copolymers determined experimentally and predicted theoretically by the Fox equation.

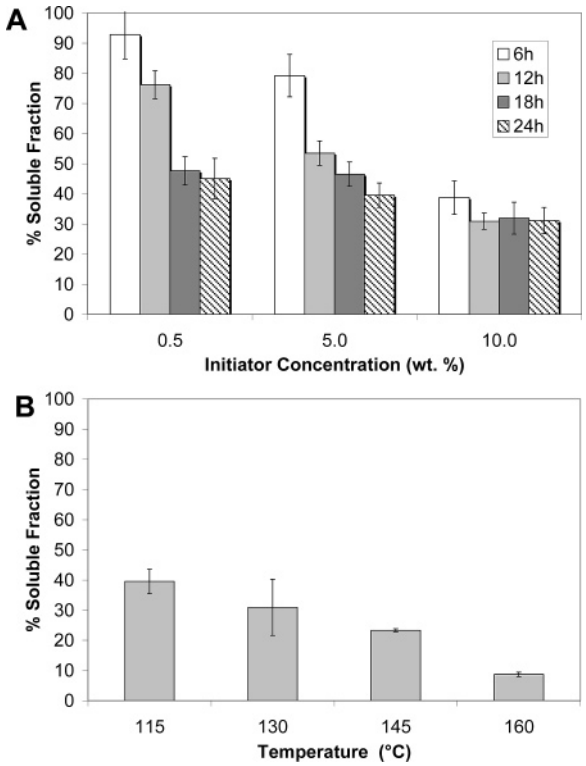

Figure 4. The effect of (A) BPO concentration and curing time at 115 °C, and (B) curing temperature on the soluble fraction of the elastomer materials prepared from prepolymer **1**.

of different free radical initiators was investigated. Third, vinyl monomers, such as *N*-vinyl pyrrolidone (NVP), were mixed with the linear amorphous prepolymer during cross-linking.

Indeed, cross-linking of the copolymeric prepolymers afforded elastomers with a broad range of mechanical properties. The prepolymers were cross-linked using similar curing conditions of 5.0 wt % BPO for 24 h at 130 °C. The mechanical and thermal properties of the resulting elastomers correlated well with the amount of HMA in the material (Table 4). The Young's modulus steadily increased as the amount of HMA in the material increased, ranging from 0.01 to 0.4 MPa, while the materials demonstrated ultimate elongations over 170%. Correspondingly, the cross-linking density increased and soluble fraction decreased as the amount of HMA in the material increased.

Having investigated the use of copolymeric prepolymers to modify the mechanical and thermal properties of the elastomeric materials, the effect of the radical initiator was investigated. A second commonly used radical initiator, 2,2′-azobis(2-methyl-

Table 3. Effect of Ethylene Glycol Oligomer Length and BPO Concentration on Thermal and Mechanical Properties of Elastomers Prepared from Prepolymers **1**−**3** Cured at 130 °C for 24 h

			weight loss (°C)[b]		G	ϵ	σ	ν	
elastomer	EG	T_g (°C)[a]	5%	10%	(MPa)[c]	(MPa)[c]	(%)[c]	(mmol/L)[c]	Q_s (%)[d]
1	2[e]	−13	285	309	0.3	0.2	122	43.1	30
2	2[f]	−13	270	293	0.5	0.4	89	63.2	26
3	2[g]	−11	275	299	0.4	0.4	92	49.8	27
4	3[g]	−21	273	296	0.3	0.2	98	36.3	20
5	4[g]	−22	274	295	0.2	0.1	127	20.9	21
6	2[h]	−10	268	298	0.4	0.5	93	65.1	24

[a] Determined by DSC, second heat, 10 °C/min. [b] Determined by TGA in N_2, 10 °C/min. [c] Determined by Instron, 20 mm/min crosshead speed. [d] Extracted in methylene chloride for 24 h at 25 °C. [e] 0.5 wt % BPO. [f] 10.0 wt % BPO. [g] 5.0 wt % BPO. [h] 5.0 wt % BPO, prepolymer **4**.

Table 4. Effect of the Amount of HMA in the Elastomer on the Thermal and Mechanical Properties of Copolymer Materials Cured at 130 °C for 24 h with 5.0 wt % BPO

	HMA:AA		weight loss (°C)[c]		G	ϵ	σ	ν	
elastomer	ratio[a]	T_g (°C)[b]	5%	10%	(MPa)[d]	(MPa)[d]	(%)[d]	(mmol/L)[d]	Q_s (%)[e]
7	20:80	−39	296	320	0.02	0.07	248	3	51
8	40:60	−34	299	325	0.01	0.1	300	1	41
9	60:40	−25	287	313	0.09	0.3	172	12	32
10	80:20	−14	285	307	0.2	0.3	128	27	29
11	100:0	−11	275	299	0.4	0.4	92	54	27

[a] Molar ratio. [b] Determined by DSC, second heat, 10 °C/min. [c] Determined by TGA in N_2, 10 °C/min. [d] Determined by Instron, 20 mm/min crosshead speed. [e] Extracted in methylene chloride for 24 h at 25 °C.

Table 5. Effect of AIBN Initiator on Thermal and Mechanical Properties of Elastomers Prepared from Prepolymer **1** at 130 °C for 24 h

	wt %		weight loss (°C)[b]		G	ϵ	σ	ν	
elastomer	AIBN	T_g (°C)[a]	5%	10%	(MPa)[c]	(MPa)[c]	(%)[c]	(mmol/L)[c]	Q (%)[d]
12	0.5	4	266	290	1.5	0.7	65	202	16
13	5.0	−1	262	285	1.6	0.8	63	215	18
14	10.0	−2	265	289	2.0	0.7	75	269	15

[a] Determined by DSC, second heat, 10 °C/min. [b] Determined by TGA in N_2, 10 °C/min. [c] Determined by Instron, 20 mm/min crosshead speed. [d] Extracted in methylene chloride for 24 h at 25 °C.

Table 6. Effect of NVP on Thermal and Mechanical Properties of Elastomers Using 5.0 wt % AIBN at 130 °C for 24 h

		wt %		weight loss (°C)[c]		G	ϵ	σ	ν	
elastomer[a]	EG	NVP	T_g (°C)[b]	5%	10%	(MPa)[d]	(MPa)[d]	(%)[d]	(mmol/L)[d]	Q (%)[e]
13	2	0.0	−1	262	285	1.5	0.7	65	202	18
15	2	1.0	2	275	297	3.3	1.3	140	444	18
16	2	2.0	3	271	295	8.4	1.2	124	1130	19
17	2	4.0	−10	262	288	21.5	3.0	143	2890	24
18	2	8.0	−13	265	291	10.0	1.4	138	1350	21
19	2	16.0	−13	273	299	0.8	0.7	102	108	29
20	4	0.0	−17	274	297	0.4	0.2	80	54	25
21	4	1.0	−22	273	296	0.4	0.2	75	55	32
22	4	4.0	−26	268	293	0.3	0.1	95	40	39
23	4	16.0	−27	265	289	0.2	0.2	110	27	38

[a] All elastomers were prepared from prepolymers **1** and **3**, respectively. [b] Determined by DSC, second heat, 10 °C/min. [c] Determined by TGA in N_2, 10 °C/min. [d] Determined by Instron, 20 mm/min crosshead speed. [e] Extracted in methylene chloride for 24 h at 25 °C.

propionitrile) (AIBN), was used to cure HMA:2EG prepolymers at 130 °C using initiator concentrations between 0.5 and 10.0 wt %. The use of AIBN clearly affected the properties of the materials as compared to BPO (Table 5). Glass transition temperatures of the materials were raised to near 0 °C. The Young's modulus more than doubled, ranging from 1.5 to 2.0 MPa. Accordingly, cross-linking densities increased by approximately 5 times, and soluble fractions decreased by approximately 10%. These improvements in properties can be explained by the fact that the AIBN visibly mixed more efficiently with the prepolymer.

Finally, the effect of adding *N*-vinyl pyrrolidone (NVP) to the mixture of AIBN and prepolymer was investigated. NVP was chosen because it is a reactive vinyl monomer that has precedence in the literature for being used to promote cross-linking.[38] Cross-linking conditions were 5.0 wt % of initiator at 130 °C for 24 h with varying amount of NVP added to the mixture. The addition of NVP did not have a large effect on the thermal properties of the resulting materials, with all glass transition temperatures still significantly below room temperature (Table 6). However, the mechanical properties were dramatically improved. Materials with a Young's modulus as high as 20 MPa were prepared. Correspondingly, the ultimate stress values and cross-linking densities also increased. However, there is a maximum at 4.0 wt % NVP that is reached with

(38) Berlot, S.; Aissaoui, Z.; Pavon-Djavid, G.; Belleney, J.; Jozefowicz, M.; Helary, G.; Migonney, V. *Biomacromolecules* **2002**, *3*, 63−68.

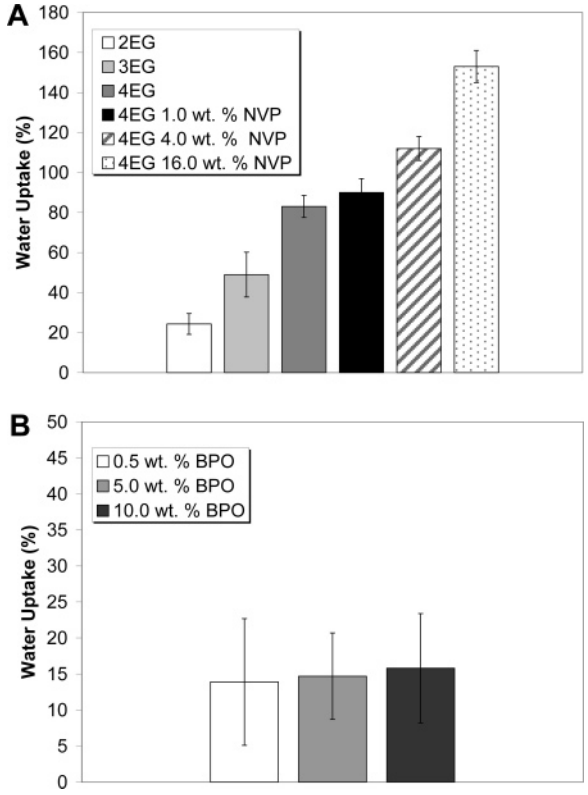

Figure 5. Variation in the equilibrium water uptake of elastomers by changing the (A) EG length of the prepolymer and amount of NVP additive, and (B) concentration of BPO used to cross-link 2EG prepolymers after samples were swollen in buffer solution for 4 days.

these improvements in mechanical properties, due to the poor tensile properties of poly(*N*-vinyl pyrrolidone).

Thus far, we have demonstrated the ability to control mechanical properties by using: (1) copolymeric prepolymers, (2) different radical initiators, and (3) additional vinyl monomers, such as NVP. Because of the synthetic versatility our methodology affords, we are able to precisely control the mechanical properties of the resulting degradable elastomers over a window of 3 orders of magnitude, with Young's moduli between 0.02 and 20 MPa. Langer[2,24] and Zhang[26] separately provide examples of the use of a polycondensation method, reacting sebacic acid and glycerol, to prepare some elegant examples of degradable elastomeric materials. The Young's moduli of these materials were in the range of 0.1−8 MPa. Ameer and Zhang also provide similar examples using citric acid as a polyfunctional acid, but the same range of mechanical properties is achieved.[25,27]

As previously discussed, it is advantageous in numerous biomedical applications that the mechanical properties of the device or scaffold be similar to the mechanical properties of surrounding tissues. Our materials have mechanical properties similar to those of elastin ($G = 0.3-0.6$ MPa, $\epsilon = 0.36-4.4$ MPa, and $\sigma = 100-220\%$) and subsequently elastin-rich tissues such as ligaments and vascular walls.[39] The ultimate extension of our materials is approaching that of arteries and veins (<220%) and is significantly larger than that of tendons (<18%).[2] Furthermore, the Young's modulus and tensile strength values of smooth muscle are very similar to those of our materials.

(39) Puskas, J. E.; Chen, Y. *Biomacromolecules* **2004**, *5*, 1141−1154.

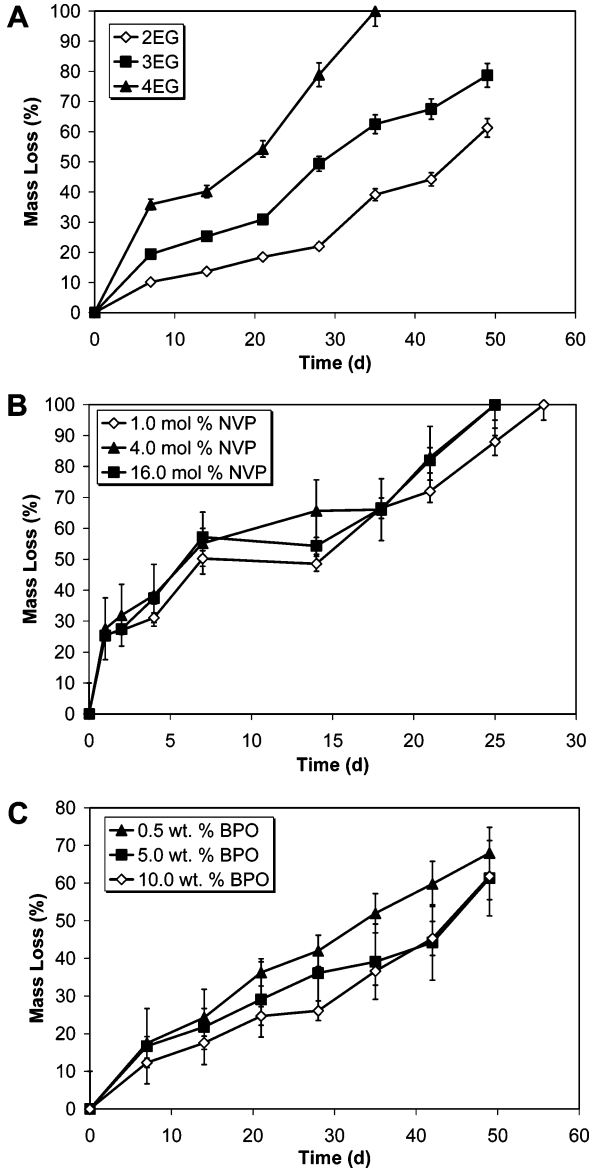

Figure 6. The effect of the (A) EG oligomer length used to prepare the prepolymer, (B) amount of NVP added, and (C) concentration of BPO used to cross-link the 2EG prepolymer on the mass loss of the elastomers.

Once the ability to tune the thermal and mechanical properties of the materials within a wide range of values was demonstrated, the ability to precisely control the water uptake and degradation rates of the elastomers was investigated. It is intuitive that using a longer EG oligomer or more NVP will make the material more hydrophilic, affecting its water uptake properties. The data in Figure 5 indeed demonstrate that the equilibrium water uptake properties of the materials differ greatly depending on these variables. Materials prepared from the three different EG oligomer lengths show statistically different water uptake levels, with the level increasing as the EG oligomer length increases. Materials prepared from 4EG show the largest uptake, above 80%, while materials prepared from 2EG show the smallest uptake, near 20% (Figure 5A, first three entries). NVP also affected the water uptake, with HMA:4EG materials with 16.0 wt % NVP added, demonstrating water uptake levels near 160%, twice that of HMA:4EG (Figure 5A, last three entries). The effect of initiator concentration on water uptake was also

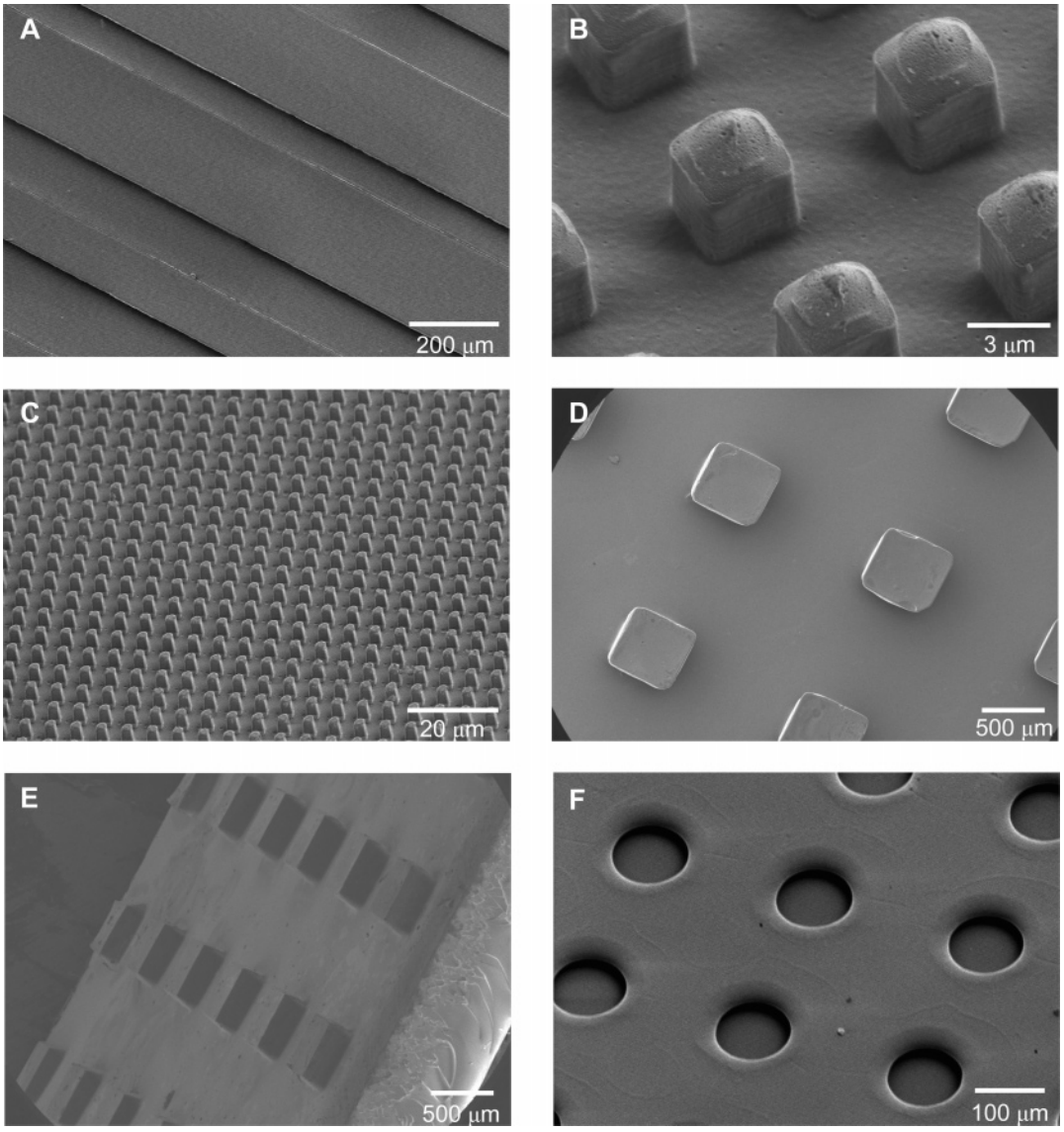

Figure 7. SEM images of fabricated degradable elastomeric micropatterned embossed surfaces: (A) 50−175 μm groove embossed film. (B) 3 × 3 × 3.7 μm square embossed film. (C) 3 × 3 × 7.9 μm square embossed film. (D) 500 × 500 × 500 μm square embossed film. (E) End-on-view of micropatterned 500 × 500 × 500 μm square embossed film. (F) 80 μm diameter cylindrical holes.

Table 7. Rate of Mass Loss of Elastomers[a]

elastomer	wt % NVP	k_{mass} (% loss/d)
2EG[b]	0	1.1
3EG[b]	0	1.7
4EG[b]	0	2.8
2EG[c]	0	1.5
2EG[d]	0	1.2
2EG[b,e]	1.0	2.6
2EG[b,e]	4.0	2.7
2EG[b,e]	16.0	2.7

[a] Zero-order rate determined by plotting (% mass loss) versus *t* and fitting the data with a linear regression (see Supporting Information, Figure S1). [b] 5.0 wt % BPO, 130 °C, 24 h. [c] 0.5 wt % BPO, 130 °C, 24 h. [d] 10.0 wt % BPO, 130 °C, 24 h. [e] Data from first 6 days excluded from regression (see Supporting Information, Figure S1).

investigated. Water uptake values of elastomers **1**−**3** prepared from prepolymer **1** were nearly identical (Figure 5B). While several materials demonstrate final equilibrium water uptake levels similar to those of hydrogel materials, the kinetics of the uptake are orders of magnitude less than typical hydrogels (days as opposed to hours). All materials evaluated demonstrated similar swelling kinetics regardless of EG length or degree of cross-linking.

Given the broad range of water uptake values, significant differences in the degradation rates were predicted. The degradation properties were characterized by measuring the loss of mass of the elastomers over time (Figure 6). Several observations with regard to the mass loss of the elastomers were noted. First, all materials demonstrated an initial rapid loss in mass. Second, the EG oligomer length had a significant effect on the mass loss of the elastomers (Figure 6A). Both the percent and the rate of mass loss increased as the length of the EG oligomer increased (Table 7). Materials prepared from 4EG prepolymers degraded the most rapidly, with complete degradation occurring in 30 days (Figure 6A). Finally, the concentration of initiator and NVP used to prepare the cross-linked elastomers did not have a significant effect on the rate of degradation of the materials (Figure 6B and C).

To our knowledge, there exists only one other example of a bioelastomer material that degrades this rapidly.[25] The sebacic acid glycerol materials previously discussed demonstrate 20%

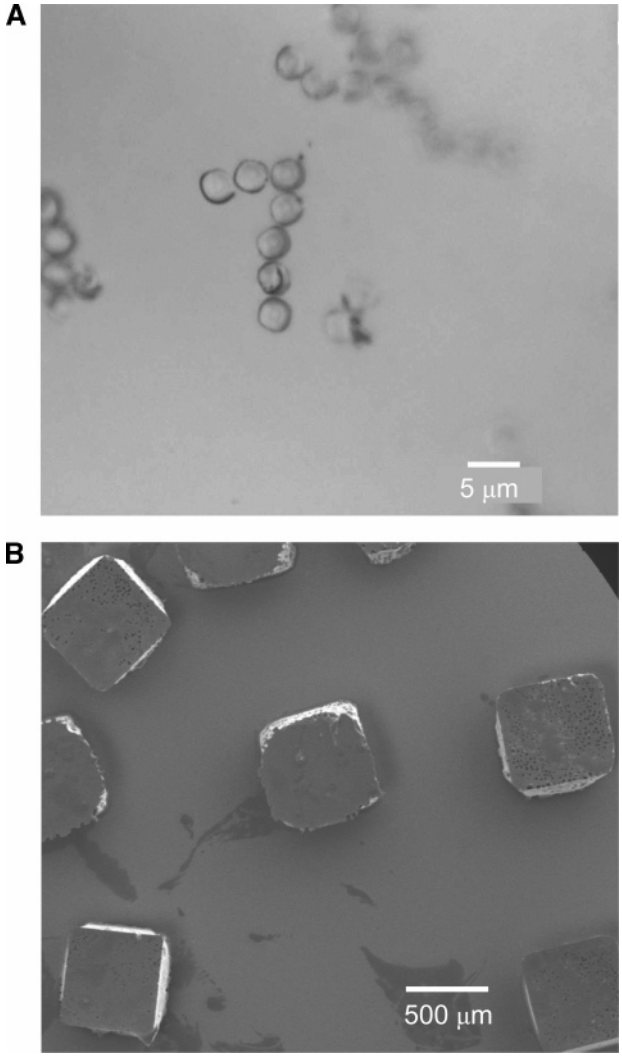

Figure 8. SEM images of (A) 3 and (B) 500 μm particles fabricated using PRINT techniques.

mass loss after 60 days.[2] Similar citric acid-based materials require up to 25 weeks to degrade.[27] Not surprisingly, any of the degradable elastomer materials that rely on crystalline poly(L-lactic acid) or poly(ϵ-caprolactone) require significantly longer degradation periods. Some materials, in fact, demonstrate only 20% weight loss after 40 weeks.

A key feature of this hybrid approach is the array of processing options that are available as a result of the liquid prepolymers. It can be argued that the fabrication of these prepolymers rivals the utility and ease of fabrication of silicone materials, with the benefit of providing a degradable material. The few examples in the literature of fabricated degradable elastomeric devices require more than 6 days to fabricate and are limited in their processing options as compared to our materials.[34] In contrast, our liquid prepolymers can be easily fabricated into a wide range of devices in less than 24 h. To demonstrate the utility and flexibility of the processing options available to our materials, four different classes of shape-specific, biologically relevant structures were fabricated. First, a variety of two-dimensional monolithic shapes were fabricated, including squares, disks, and rings, by simply using the appropriate shape-specific mold. Second, three-dimensional tube devices that were 4 mm in diameter were constructed using standard molding techniques. Next, the fabrication of devices with smaller feature sizes was investigated.

This ease of fabrication is especially advantageous for applications that require the molding of devices with microsized features. One such application is in tissue engineering where scaffold devices, which function as a surrogate extra cellular matrix, need to be fabricated. The shape and size of the features of these scaffolds play a very important role in controlling cellular orientation and proliferation.[40,41] To further demonstrate the flexibility in processing options of our materials, a variety of these shape-specific scaffolds were fabricated. Microporous scaffolds were fabricated using standard particle leaching techniques. Most of these types of scaffolds that are used today employ PLA or PGA, which are crystalline and lack mechanical stability. Our method affords a porous material that is both elastomeric and degradable in nature.

Besides microporous scaffolds, micropatterned surfaces are used extensively for tissue regeneration. Micropatterning is used to influence cell attachment, migration, orientation, and cellular processes.[42,43] Physical micropatterned surfaces allow for the control and manipulation of fundamental cell−substrate and cell−cell interactions. A wide variety of patterns have been investigated, including grooves, hexagons, and cylinders.[44] To date, these micropatterned surfaces have been primarily fabricated from nondegradable substrates using reactive ion etching or microcontact printing. Degradable substrates are chemically incompatible with reactive ion etching techniques, and lack the mechanical strength required for microcontact printing. Mallapragada provides one of the few examples of degradable, micropatterned surfaces, although high-pressure contact molding techniques were required and semicrystalline materials are used.[45,46] Other examples require extended fabrication times as previously described.[34]

Using standard imprint lithographic techniques, we have prepared a variety of novel size- and shape-specific degradable micropatterned embossed film surfaces (Figure 7). These micropatterned surfaces are analogous to the size and shape of micropatterned surfaces currently used in tissue engineering applications. Surfaces with grooves ranging from 50 to 175 μm wide and 10 μm deep were fabricated (Figure 7A). Similarly, surfaces with micropatterned squares on the surface were prepared (Figure 7B and C). These squares were 3×3 μm, with feature heights of 3.7 and 7.9 μm. Larger 500 μm square embossed films were also fabricated (Figure 7D and E). Finally, surfaces with disk-shaped holes 80 μm in diameter and 40 μm deep were fabricated (Figure 7F).

As a final example to demonstrate the fabrication flexibility that our materials afford, PRINT techniques described by DeSimone et al. were used to fabricate monodisperse, shape-specific particles.[47] Particle devices are necessary for many advanced drug delivery, targeting, and recognition applications. Both 3 and 500 μm cubic particles were successfully fabricated (Figure 8).

(40) Hollister, S. *Nat. Mater.* **2005**, *4*, 518−524.
(41) Wu, L.; Ding, J. *J. Biomed. Mater. Res.* **2005**, *75A*, 767−777.
(42) Magnani, A.; Priamo, A.; Pasqui, D.; Barbucci, R. *Mater. Sci. Eng.* **2003**, *23C*, 315−328.
(43) Schmalenberg, K.; Uhrich, K. *Biomaterials* **2005**, *26*, 1423−1430.
(44) Recknor, J.; Recknor, J.; Sakaguchi, D.; Mallapragada, S. *Biomaterials* **2004**, *25*, 2753−2767.
(45) Miller, C.; Jeftinija, S.; Mallapragada, S. *Tissue Eng.* **2002**, *8*, 367−378.
(46) Miller, C.; Shanks, H.; Witt, A.; Rutkowski, G.; Mallapragada, S. *Biomaterials* **2001**, *22*, 1263−1269.

Finally, given the potential use of these materials for biomedical applications, the cytotoxicity characteristics of these materials were tested. A minimum essential medium elution test was performed on all prepolymers and cross-linked elastomer materials. The materials were extracted with a minimal essential medium for 24 h at physiological conditions. The extracts were then placed on monolayers of L929 mouse fibroblast cells from the ATCC cell line. Materials were scored after 48 h. All prepolymer materials had toxicity scores of 0.0, indicating no cytotoxic response. The elastomer materials were tested before and after the soluble fraction had been removed with methylene chloride. Both materials scored 0.0, indicating no cytotoxic response. While these results indicate the possibility of biocompatibility, further in vivo and in vitro testing is required to adequately report these materials as biocompatible.

Conclusions

This liquid amorphous linear prepolymer approach is a highly versatile method for the production of degradable elastomeric materials with easily tailorable mechanical and degradation properties. To our knowledge, no examples that combine this ease of property control with the ease of fabrication exist. Because of their amorphous nature, these materials can be designed to degrade very rapidly (less than 30 days). However, materials with longer-term degradation rates (60% mass loss in 8 weeks) were also demonstrated. Furthermore, the mechanical properties of these materials can be tuned over a broad range to specifically align with multiple natural tissues. Finally, the liquid nature of the prepolymers allows for facile fabrication into multiple forms. The shapes and patterns chosen in this work were engineered nonarbitrary shapes, but these amorphous liquid prepolymers could be used to fabricate degradable elastomeric devices based on shapes found in nature, such as viruses, cells, or proteins. By combining the control over mechanical and degradation properties with the ease of fabrication, this method allows for the rational design of shape-specific devices that possess specific targeted properties.

Acknowledgment. We would like to thank Professor Muhammad N. Yousaf and Eugene Chan for the use of micropatterned molds. This material is based upon research funding by the National Science Foundation (Department of Materials Research) under grant 0418499. It is also supported by The University of North Carolina at Chapel Hill-Startup Funds and partial support from the National Science Foundation-Science and Technology Center (5-37503) and the Carolina Center for Cancer Nanotechnology Excellence from the National Cancer Institute.

Supporting Information Available: Full experimental details as well as kinetics plots for degradation experiments. This material is available free of charge via the Internet at http://pubs.acs.org.

JA063092M

(47) Rolland, J.; Maynor, B.; Euliss, L.; Exner, A.; Denison, G.; DeSimone, J. M. *J. Am. Chem. Soc.* **2005**, *127*, 10096−10100.